WEP Warwick Evans Publishing

Transactions on Engineering and Technology Research
ISSN: 2960-1797, eISSN: 2960-2246 | Volume 2
AMMEE 2024

Research on Axial Compression Test and Finite Element Analysis of Sea Sand Concrete Filled CFRP-Steel-CFRP Composite Circular Tubular Stub Column

Guihan Peng[1,a], Liqiong Yu[1,b], Baomin Yao[2,c], Huiling Luo[3,d*]

[1]Civil Engineering College of Fuzhou University Fuzhou Fujian, China

[2]China Nuclear Industry 24 Construction Co., Ltd. Mianyang Sichuan, China

[3]School of Applied Science and Engineering, Fuzhou Institute of Technology, Fuzhou Fujian, China

[a]908840471@qq.com, [b]ylq110831@163.com, [c]pgh1998@163.com, [d]lhl_202006@163.com

Abstract. In order to study axial pressure performance of sea sand concrete filled CFRP-steel-CFRP composite circular tubular stub column, the finite element model of composite constrained short column was established by using ABAQUS, based on experimental research. The accuracy of the finite element model was validated by comparing the finite element with the experimental data. Furthermore, the influence of the number of CFRP layers, the tensile strength of CFRP and the thickness of steel tube on the mechanical properties of components was explored. Finally, the applicability of the existing algorithms for bearing capacity was discussed and a simplified calculation formula was proposed. The results indicate that the structural parameters are directly proportional to the bearing capacity of the components, and the increase of CFRP layers is the most significant. With the increase of CFRP layers, the stiffness of the linear strengthening section of load-displacement curve can also be significantly improved. The existing relevant bearing capacity algorithms are relatively conservative for the combined structure, and the simplified calculation formula presented in this paper has little deviation from the experimental value.

Keywords: CFRP, sea sand concrete-filled steel tube, finite element simulation, axial compression test.

1. Introduction

With the advantages of high bearing capacity, good ductility and convenient construction, concrete-filled steel tube structure is widely used in various building structures. Domestic and foreign scholars have also carried out a lot of relevant research work on concrete-filled steel tube structures. With the rapid development of our economy, as one of the main raw materials of concrete, river sand is increasingly in shortage. Thanks to the long coastline of our country, we have the rich sea sand resources. While in order to make full use of sea sand, it is necessary to find a reasonable and effective way to reduce the corrosion of steel by chloride ions in sea sand. FRP material not only has excellent corrosion resistance, but also has the advantages of high tensile strength and light weight, among which the CFRP composite material is most widely used. Therefore, the CFRP composite material is applied to sea sand concrete-filled steel tube to form the sea sand concrete filled CFRP-steel-CFRP composite tube structure. The new combination structure can not only effectively avoid structural corrosion, alleviate the lack of river sand, but also have superior properties such as high strength.

Currently, extensive research has been conducted by scholars both domestically and internationally on the structural behavior of CFRP-concrete-filled steel tube systems. The research of Gu Wei[1] and Xiao[2] indicates that CFRP constraint can significantly improve the axial pressure capacity of concrete-filled steel tube structure. The bearing capacity is still higher than that of the same CFST specimen even after the CFRP is broken and withdrawn from work. Mukherjee A[3] and Tao[4] discovered that CFRP imposes more stringent constraints on circular concrete columns, leading to a

significant enhancement in their load-bearing capacity. Conversely, square and rectangular columns are susceptible to brittle fracture at the corners.

However, the majority of existing studies have primarily focused on coating CFRP on the outer wall of steel tubes, with limited attention given to coating CFRP on the inner wall. Therefore, this study conducted axial compression tests on sea sand concrete filled CFRP-steel-CFRP composite circular tubular stub column. Based on these test results, a finite element model was established using ABAQUS to analyze the effects of various factors such as the number and position of CFRP layers, tensile strength of CFRP, thickness of steel tubes, fiber winding angle, and type of FRP on the mechanical properties of such structures.

2. The Experimental Study

A total of 26 short columns were designed to investigate the axial compressive properties of sea sand concrete filled CFRP-steel-CFRP composite circular tubular stub columns, comprising 19 specimens with sea sand concrete filled CFRP-steel-CFRP composite circular tubular stub columns, 6 specimens with sea sand concrete-filled steel circular tubular stub columns, and 1 specimen with concrete-filled steel circular tubular stub column. The steel tubes used in the test had an outer diameter of 150mm and a height of 450mm, made from two types of steel: Q235 and Q345. Fig. 1 shows the test components.

Experimental design parameters included number and position of CFRP layers, thickness of steel tubes, yield strength of steel tube, and compressive strength of concrete.

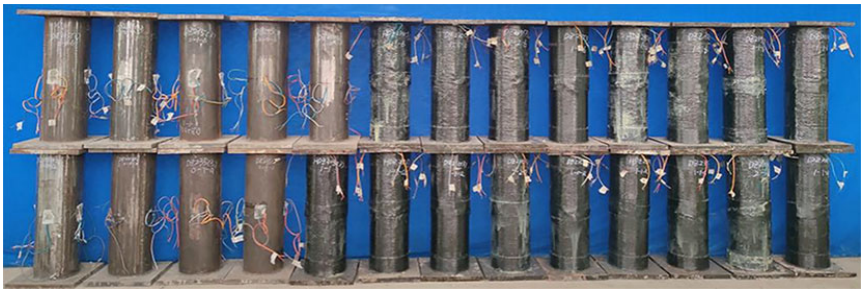

Fig.1 Test components

3. Establishment of The Finite Element Model

3.1 Material Constitutive Structure and Model Parameters

The finite element model was established using Abaqus, where a total of 6,321 elements and 11,128 nodes were employed. The constitutive model for steel incorporates the five-stage stress-strain relationship proposed by Han Linhai[5]. For sea sand concrete, the same confined concrete material constitutive model as river sand concrete of equivalent grade was adopted. Referring to Wang Qingli's modified stress-strain relationship for circular CFRP-steel tube confined concrete in ABAQUS[8], the failure energy criterion for concrete[9] was utilized to simulate tensile behavior. The Hashin damage parameters were utilized in accordance with the Hashin failure criterion to simulate the progressive development of damage and eventual failure process of linear elastic CFRP material. The damage was realized through the stiffness degradation of the material.

In this finite element model, S4R shell elements were used to represent the steel tube while C3D8R 3D solid units simulated the core concrete. SC8R continuous shell elements were employed to design the CFRP composite with a local coordinate system defining its thickness. Hard contact was assumed between steel tube and concrete with Coulomb friction governing tangential contact which friction coefficient μ is 0.60. Tie binding represented the interaction between CFRP and steel tube. Hard contact existed between CFRP and inner wall of steel tube. End plate exhibited binding contact with steel tube and normal hard contact with top surface of concrete[10]. Only Uz degrees of freedom in

vertical loading direction were released in this model while other degrees of freedom remained constrained. Displacement control method was adopted for loading where displacement load was applied at center position on upper end plate of specimen. The specific finite element model is shown in Figure 2.

Table 1 List of Parameters of Axial Compression Short Column Specimens

Specimen number	D×ts/mm×mm	L/mm	fy/MPa	fcu/MPa	tcf/mm	Nue/kN
DZ235(3)-1-0a	150×3	450	319.95	57.1	0.167	2028.19
DZ235(3)-1-0b	150×3	450	319.95	57.1	0.167	2261.74
DZ235(3)-0-1a	150×3	450	319.95	57.1	0.167	2257.55
DZ235(3)-0-1b	150×3	450	319.95	57.1	0.167	2362.87
DZ235(3)-1-1a	150×3	450	319.95	57.1	0.334	2704.62
DZ235(3)-1-1b	150×3	450	319.95	57.1	0.334	2846.96
DZ235(3)-2-1a	150×3	450	319.95	57.1	0.501	3104.42
DZ235(3)-2-1b	150×3	450	319.95	57.1	0.501	3275.79
DZ235(3)-2-2a	150×3	450	319.95	57.1	0.668	3342.53
DZ235(3)-2-2b	150×3	450	319.95	57.1	0.668	3399.19
HDZ235(3)-1-1a	150×3	450	319.95	62.9	0.334	2758.71
HDZ235(3)-1-1b	150×3	450	319.95	62.9	0.334	2826.67
DZ235(5)-1-1a	150×5	450	281.23	57.1	0.334	3208.85
DZ235(5)-1-1b	150×5	450	281.23	57.1	0.334	3162.53
HDZ235(5)-1-1a	150×5	450	281.23	62.9	0.334	3301.57
HDZ235(5)-1-1b	150×5	450	281.23	62.9	0.334	3259.19
DZ345(3)-1-1a	150×3	450	396.32	57.1	0.334	3006.52
DZ345(3)-1-1b	150×3	450	396.32	57.1	0.334	3004.06
HDZ345(3)-1-1	150×3	450	396.32	62.9	0.334	3128.59

Test results for bearing capacity are presented in Table 1; DZ indicates C50 concrete while HDZ indicates high-strength concrete. For example, DZ235(3)-2-1b represents a specimen made using Q235 carbon steel with a wall thickness of 3mm. The first number 2 after "-" represents there is two layers on its outer surface and the second number 1 means one layer on its inner surface. The letter "b" denotes this component as part b within a group consisting two components.

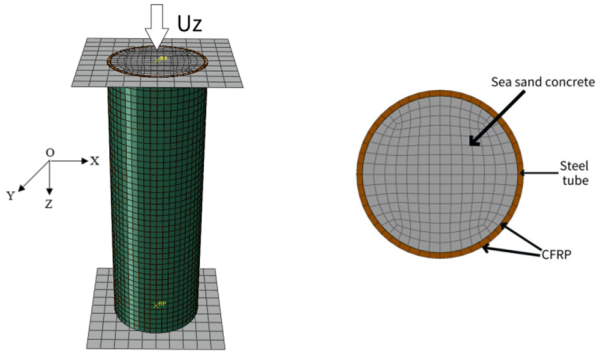

Fig.2 Finite element model

3.2 Validation of the Finite Element Model

The comparison of component failure modes and partial load-displacement curves (*N-Δ*) between the test and the finite element model is illustrated in Figure 3. As depicted in the Figure, both experimental and finite element simulation results demonstrate that the outermost CFRP layer experiences tensile failure first, while no evident local buckling occurs in the steel tube itself, indicating effective inhibition of buckling deformation by external CFRP reinforcement. Moreover, the load-displacement curves of both exhibit similar development trends with peak loads falling within an acceptable error range, except for variations observed in the declining section. This discrepancy can be attributed to idealization of component properties and mutual contact relations after CFRP fracture during finite element simulation.

By comparing the ultimate bearing capacity obtained from finite element simulation with experimental results, NFE/Nue is determined as a measure. Table 2 presents partial numerical comparison results. After calculation, NFE/Nue yields a mean value of 0.993 with a standard deviation of 0.035. The finding indicates excellent agreement between failure modes, load-strain curves, and ultimate bearing capacity obtained through finite element simulation and experimental observations, thus validating high accuracy of our established finite element model for further analysis on specimen mechanisms and parameters.

4. Finite Element Analysis

Considering the limitations and contingencies of experimental studies, a finite element model was employed to investigate key parameters influencing the mechanical properties of sea sand concrete filled CFRP-Steel-CFRP composite axial compression circular tubular stub column. These parameters include the number of CFRP layers, CFRP paste position, tensile strength of CFRP, steel tube thickness, fiber winding angle, and type of FRP.

4.1 CFRP Parameters

The influence of CFRP related parameters on the load-displacement (N-Δ) curve and ultimate bearing capacity is illustrated in Figure 4 and 5. By examining Figure 4(a) and Figure 5(a), it can be observed that when employing the control variable method to alter a single parameter, an increase in CFRP mono layer thickness significantly enhances the ultimate bearing capacity of the structure. However, there are no significant changes in the overall shape of the load-displacement curve or elastic stage stiffness; only the quadratic stiffness of the linear reinforcement segment increases. As depicted in Figure 5(c), increasing the number of CFRP layers has a notable impact on structural bearing capacity, with each additional layer providing a relatively stable enhancement at approximately 50%. Comparatively, both increasing CFRP layers and augmenting single-layer thickness improve structural bearing capacity. Nevertheless, modeling analysis reveals substantial differences among various types of FRP materials due to brittle characteristics exhibited by CFRP. Increasing either single-layer thickness or adding more layers leads to reduced component ductility. Furthermore, altering CFRP tensile strength has a far less pronounced effect on structural bearing capacity

compared to variations in CFRP thickness, and the overall shape of the component, the stiffness of the elastic stage and the stiffness of the linear reinforcement segment are also little affected, as evident from Figure 4(b) and Figure 5(b). When increasing fiber winding angle, as shown in Figure 4(c), there is no increase observed in structural load-displacement curve stiffness, indicating minimal constraint imposed by fibers at higher winding angles. Notably, when reaching a winding angle of 45 degrees, linearity within reinforcement curves tends to be gentle, indicating that the fiber has little constraint effect on the component at this time. Therefore, if applied to practical engineering, it is advisable to avoid a high winding angle and instead opt for a ring arrangement as much as possible.

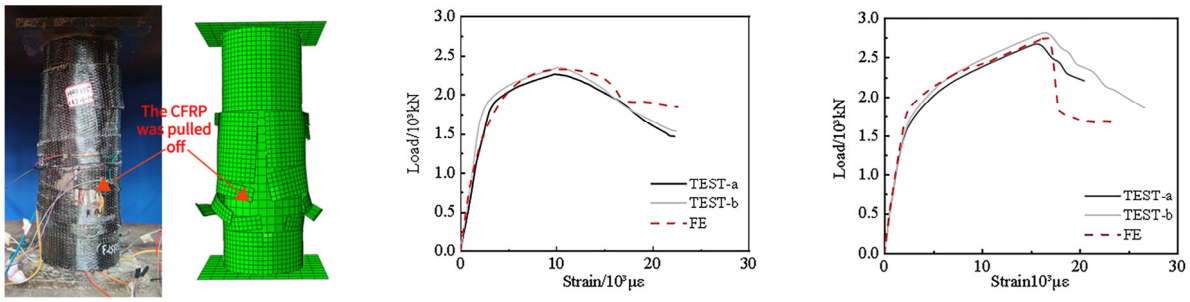

(a)failure mode (b)DZ235(3)-0-1 (c)DZ235(3)-1-1

Fig.3 Comparison of failure modes and N-Δ curves on test and simulation

Table 2 Comparison of Finite Element and Test on Ultimate Bearing Capacity

specimen number	Nue(kN)	NFE(kN)	NFE/ Nue
DZ235(3)-0-1a	2257.55	2263.77	1.003
DZ235(3)-0-1b	2362.87	2263.77	0.958
DZ235(3)-1-1a	2704.62	2769.17	1.024
DZ235(3)-1-1b	2846.96	2769.17	0.973
DZ235(3)-2-1a	3104.42	3269.07	1.053
DZ235(3)-2-1b	3275.79	3269.07	0.998
DZ235(3)-2-2a	3342.53	3400.51	1.017
DZ235(3)-2-2b	3399.19	3400.51	1.000

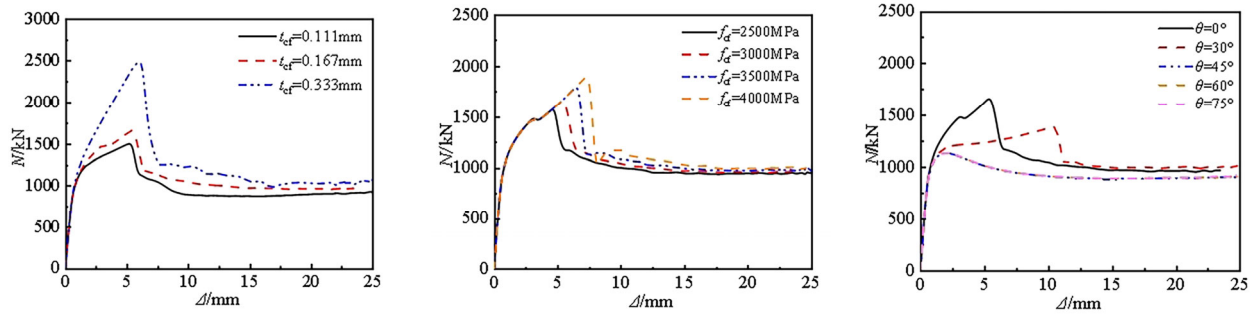

(a)CFRP thickness (b)CFRP tensile strength (c)fiber winding angle

Fig.4 Effect of CFRP parameters on structural N- Δ curves

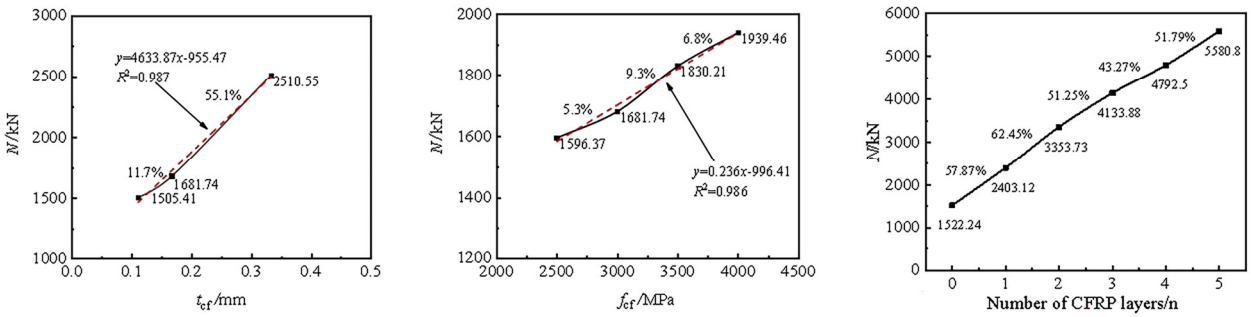

(a)CFRP thickness (b)CFRP tensile strength (c)number of CFRP layers

Fig.5 Effect of CFRP parameters on structural ultimate bearing capacity

The partial finite element detailed parameters of composite constrained stub column are presented in Table 3, where tcf represents CFRP thickness, ts denotes steel tube thickness, fcf signifies CFRP tensile strength, fy indicates yield strength of steel tube. The number of fiber cloth layers on the outside and inside of the steel pipe is denoted as ncf,o and ncf,i respectively. And ΔNFE refers to the increase in ultimate bearing capacity for each corresponding component. DZFE-2 and DZFE-3 are variations from DZFE-1, while DZFE-5 and DZFE-6 contrast with DZFE-4.

According to the calculation results of ΔNFE in the table, it is evident that there exists a significant disparity in the enhancement effect on the ultimate bearing capacity of steel tube members when fiber cloth is applied internally or externally. Taking DZFE-1 as the control specimen without any fiber cloth on its inner and outer walls. DZFE-2 incorporates an additional layer of fiber cloth on the outer wall of the steel tube, the calculation results demonstrate a 39.75% increase in ultimate bearing capacity for this component. While by adding a layer of fiber cloth to the inner wall of the steel tube, it can be observed that structural load-bearing capacity of DZFE-3 augmented by 52.73%. Similarly, when using DZFE-4 as the control specimen with both inner and outer walls coated with a layer fiber cloth, adding a layer of fiber cloth to its outer wall like DZFE-5 leads to only a 9.46% increase in steel tube bearing capacity. However, incorporating a layer of fiber cloth on its inner wall yields an increased bearing capacity by 19.01%, according to the DZFE-6.Furthermore, by comparing DZFE-2, DZFE-4, and DZFE-6, if maintain a constant layer of fiber cloth on the outer wall of the steel tube, the bearing capacity increases by 12.96% when the number of fiber layers pasted inner wall ranges from 0 to 1 and by 21.47% from 1 to 2. For DZFE-3, DZFE-4, and DZFE-5, keeping a layer of fiber cloth on the inner wall of the steel tube unchanged, increasing the number of fiber layers on the outer wall from 0 to 1 and from 1 to 2 results in only a improvement of 3.36% and 9.78% in bearing capacity, respectively.

In summary, increasing the number of CFRP layers improves the ultimate bearing capacity of a member whether it is applied on the inner or outer wall of a steel tube. However, the position where CFRP is applied affects its

Table 3 Detailed Parameters of Short Column Finite Element

serial number	tcf(mm)	ts(mm)	fcf(MPa)	fy(MPa)	ncf, o	ncf, i	NFE(kN)	ΔNFE
DZFE-1	0.167	3	2500	355	0	0	1522.24	—
DZFE-2	0.167	3	2500	355	1	0	2127.34	39.75%
DZFE-3	0.167	3	2500	355	0	1	2324.95	52.73%
DZFE-4	0.167	3	2500	355	1	1	2403.12	—
DZFE-5	0.167	3	2500	355	2	1	2630.42	9.46%
DZFE-6	0.167	3	2500	355	1	2	2859.91	19.01%
DZFE-7	0.167	3	2500	355	2	2	3353.73	—
DZFE-8	0.167	3	2500	355	3	3	4133.88	—
DZFE-9	0.167	3	2500	355	4	4	4792.5	—
DZFE-10	0.167	3	2500	355	5	5	5580.8	—

impact on bearing capacity differently. Based on data analysis results, applying CFRP to the inner wall of steel tube has a greater effect than applying it to the outer wall. Calculations show that adding one layer of CFRP to the inner wall increases bearing capacity by approximately 10% more than adding one layer to the outer wall.

Stress time-history curve analysis reveals that concrete failure in concrete-filled steel tube structures occurs earlier than steel tube yield. In composite columns made from CFRP-steel-CFRP tubes, CFRP breaks first followed by concrete collapse and finally yielding of steel tubes. Compared with concrete-filled steel tube, pasting CFRP outside the steel tube advances its yield point but has little effect on yield time point for concrete. When pasted inside the steel tube, stress yield points for both materials advance towards CFRP stress yield points and all three materials fail at similar times. It indicates that stronger synergistic effects between CFRP, steel tube and concrete exist when pasting CFRP on the

inner wall of steel tube. Therefore, applying CFRP to the inner surface produces stronger hoop effects and greater structural bearing capacity improvements.

4.2 Other Parameters

Fig. 6 and 7 illustrate the impact of steel tube thickness, steel yield strength, and concrete strength on the load-displacement (N-Δ) curve and ultimate bearing capacity of composite constrained short columns. As shown in Fig.6 and 7 (a), increasing the steel tube thickness from 3mm to 6mm results in a respective increase of 13.9%, 10.8%, and 10.6% in the ultimate bearing capacity for each additional millimeter increment. The stiffness and yield strength of the load-displacement curve exhibit some enhancement during the elastic stage, while the stiffness of the linear strengthening section remains relatively unchanged. To study the influence of steel tube yield strength fy, taking 235MPa as the control group. It can be observed from Fig.6 and 7 (b) that when fy increases to 345MPa, 420MPa, and 550MPa respectively, the corresponding ultimate bearing capacity increases by 16.1%, 25.6%, and 41.2%. Additionally, the load-displacement curve exhibits a similar trend as the change in steel tube thickness. In comparison to concrete with a strength of 30MPa, it can be seen from Fig.6 and 7 (c) that increasing the concrete strength to 50MPa, 70MPa, and 80MPa leads to an increase in ultimate bearing capacity by7.5%,19 .4% ,and23 .7% respectively, while the load-displacement curve remains relatively unchanged. The findings indicate that the ultimate bearing capacity of the member is directly proportional to both the thickness of the steel tube and its yield strength as well as the strength of concrete. Increasing either the thickness or yield strength of the steel tube can improve the yield strength of the member to a certain extent. However, the change in these parameters has minimal impact on the overall shape of the load-displacement curve and the stiffness of the linear strengthening section.

5. Simplification of Existing Bearing Capacity Algorithms

The ultimate bearing capacity and ductility of the concrete filled CFRP-steel composite tubular column are enhanced due to the simultaneous application of lateral pressure by CFRP and steel tube on the inner core concrete, resulting in a "double hoop action". Currently, existing calculation methods for determining the ultimate bearing capacity of such structures primarily rely on formulas proposed by Wang Qingli etal.[11], Zhang Changguang etal.[12], Tao etal.[13], Gu Wei etal.[14], Lu Yiyan etal.[15] and Wei etal.[16]. Based on them and the results of 229 finite element models, with considering parameters such as the constraint effect coefficient of steel tube ξs, the constraint effect coefficient of CFRP on the outer wall ξcf,o, the constraint effect coefficient of CFRP on the inner wall ξcf,i, and the axial compressive strength of concrete fck, we obtain an index for evaluating the axial compressive strength fsc of sea sand concrete filled CFRP-steel composite tubular stub column through regression calculations. The formula (1) for calculating axial compressive capacity in sea sand concrete filled CFRP-steel composite tubular structure is as follows:

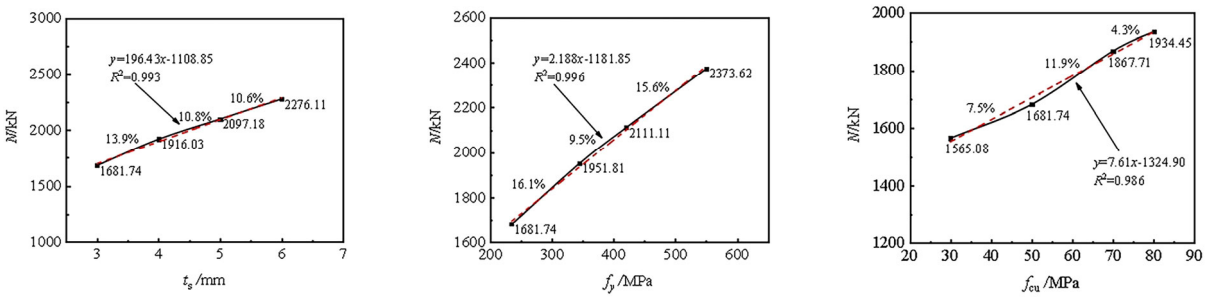

(a)steel tube thickness (b)steel yield strength (c)concrete strength

Fig.6 Effect of other parameters on structural ultimate bearing capacity

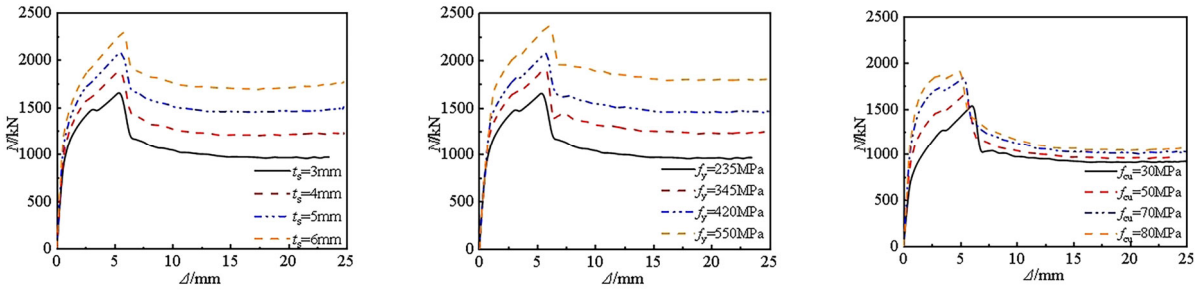

(a)steel tube thickness (b)steel yield strength (c)concrete strength

Fig.7 Effect of other parameters on structural N- Δ curves

Table 4 The Mean Value and Standard Deviation of the Ratio between the Formula and the Test Results

	NWang /Nue	NZhang /Nue	NTao/N ue	NGu/N ue	NLu/Nu e	NWei/ Nue	Nuc/Nu e
average value μ	0.939	0.919	0.842	0.977	0.901	0.875	0.994
standard deviation σ	0.062	0.078	0.047	0.096	0.047	0.055	0.049

$$N_u=[1+1.78\xi_s+1.92(\xi_{cf,o}+1.19\xi_{cf,i})]f_{ck}A_{sc} \quad (1)$$

To verify the reliability of the formula, we calculated axial compressive capacity using the same parameters for various formulas, denoted as NWang, NZhang, NTao, NGu, NLu and NWei. The axial compressive capacity calculated by the simplified formula (1) in this paper is represented as Nuc. Subsequently, all computed results were compared with the ultimate bearing capacity Nue of sea sand concrete filled CFRP-steel-CFRP composite tubular stub column measured in this study. The average value and standard deviation of each formula ratio were determined and presented in Table 4.

The calculation results in the table demonstrate that, for the sea sand concrete filled CFRP-Steel-CFRP composite axial compression circular tubular stub column structure proposed in this paper, among the existing calculation methods, Gu[14] proposed formula exhibits the closest agreement with the measured value; while it shows significant dispersion. Wang[11] and Zhang[12] bearing capacity calculation formulas rank second and yield slightly conservative results. Tao[13] formula provides the most conservative and safe prediction outcomes with smaller data discreteness. The average ratio between calculated values and test values is 0.994, with a standard deviation of 0.049. The calculated results align well with experimental values and have smaller discreteness. It means the formula is applicable to predicting the bearing capacity of similar composite tube constraint structures.

6. Conclusions

The present study investigates the behavior of sea sand concrete filled CFRP-Steel-CFRP composite axial compression circular tubular stub column. A comprehensive finite element model is developed to analyze key structural parameters, including CFRP thickness, positioning of CFRP, steel tube thickness and strength. The conclusions are summarized as follows:

(1) The ultimate bearing capacity of the member is directly proportional to the tensile strength of CFRP, steel tube thickness, yield strength of steel tube, and concrete strength. Increasing the number of CFRP layers can significantly enhance the stiffness during the linear strengthening phase of load-displacement curve. Changing the other parameters has little impact on the shape of load-displacement curve for sea sand concrete filled CFRP-Steel-CFRP composite circular tubular stub column.

(2) Among the parameters, the number of CFRP layers has the most significant impact on the bearing capacity of the member. Moreover, pasting CFRP on the inner wall of the steel tube yields a greater

effect compared to pasting it on the outer wall. The increase in bearing capacity by adding one layer of CFRP on the inner wall is approximately 10% higher than that achieved by adding one layer on the outer wall.

(3) The prediction methods for calculating bearing capacity of existing literature tend to be conservative. Among them, Gu[14] proposed calculation formula aligns best with experimental values presented in this paper; but there is considerable dispersion. Tao[13] proposed calculation formula exhibits less dispersion but lacks agreement. , In contrast, the simplified formula we proposed is relatively accurate and can be used to predict the bearing capacity of this kind of composite tubular confined concrete columns.

Acknowledgements

Fujian Province young and middle-aged teacher education research project(JAT210602)

References

[1] Gu W. Study on mechanical properties of CFRP tubular concrete column[D]. Dalian: Dalian Maritime University, 2007.

[2] Xiao Y, He W, Choi K. Confined concrete-filled tubular columns [J]. Journal of Structural Engineering, 2005, 131(03): 488-497.

[3] Mukherjee A, Boothby T E, Bakis C E. Mechanical behavior of fiber-reinforced polymer-wrapped concrete columns—Complicating effects[J]. Journal of Composites for Construction, 2004, 8(2): 97-103.

[4] Tao Z, Han L H, Zhuang J P. Axial loading behavior of CFRP strengthened concrete-filled steel tubular stub columns [J]. Advances in Structural Engineering, 2007, 10(01): 37-46.

[5] Han L H. Concrete-filled Steel Tube Structures - Theory and Practice (Third Edition)[M]. Beijing: Science Press, 2015.

[6] Huang G X, Lin Y G, Peng G H. Research on axial compression mechanical behavior of sea sand concrete filled CFRP-steel-CFRP composite steel tubular stub column[J]. Journal of Fuzhou University(Natural Science),2023,51(02):171-177.

[7] Peng G H, Luo Y P. Study on the axial bearing capacity of sea sand concrete filled stainless steel tube long columns with dumbbell-shaped section. Journal of Fuzhou University(Natural Science),2022,50(2): 222-227.

[8] Wang Q L, Zhu H F, Gao Y F. Constitutive relation of circular CFRP-steel tube restrained concrete under axial pressure[J]. Journal of Shenyang Jianzhu University(Natural Science), 2007(02): 199-203.

[9] Shen J M, Wang C Z, Jiang J J. Reinforced concrete with plate and shell finite element limit analysis[M]. Beijing: Tsinghua University Press, 1993.

[10] Yao G H. Research on working mechanism of concrete-filled steel tube member under complex stress[D]. Fuzhou: Fuzhou University, 2006.

[11] Wang Q L, Zhao C L, Zhang H B. Simplified calculation of bearing capacity of CFRP-filled steel tube short columns under axial compression[J]. Journal of Shenyang Jianzhu University(Natural Science), 2005(06): 612-615.

[12] Zhang C G, Zhao J H. Mechanical properties of CFRP-concrete-filled steel tube short axial compression columns[J]. Building Structure, 2008(03): 34-37.

[13] Tao Z, Han L H, Zhuang J P. Axial loading behavior of CFRP strengthened concrete-filled steel tubular stub columns [J]. Advances in Structural Engineering, 2007, 10(01): 37-46.

[14] Gu W. Study on mechanical properties of CFRP tubular concrete column[D]. Dalian: Dalian Maritime University, 2007.

[15] Lu Y Y, Li S, Li S. Study on axial compression behavior of FRP- round steel tube concrete short column[J]. Journal of the China Railway Society, 2016, 38(04): 105-111.

[16] Wei Y, Bai, J W, Zhang Y. Compressive behavior of high-strength seawater and sea sand concrete-filled circular FRP-steel composite tube columns[J]. Engineering Structures, 2021,240, 112357.